IEEE Robotics & Automation Magazine (RAM) paper, presented at ICRA 2026, Vienna, Austria. Cite as RAM paper.

Soft Robotic Gripper with Synergistic-Chamber Finger Module for High Force and Multi-DoF Manipulation

Sinyoung Lee, Genesung Kang, Hongmin Kim, and Dongjun Shin, *Member, IEEE*

***Abstract*— Developing a robotic hand that integrates high fingertip force, rapid response, and multi-degree-of-freedom (DoF) motion, similar to the human hand, remains a challenge in the field of robotic hands. This study presents the Soft Omni-Functional Robotic Gripper (SOFRo Gripper), designed to achieve all aforementioned characteristics. The finger module of the SOFRo Gripper incorporates synergistically arranged chambers together with a multi-node tendon routing strategy that distributes actuation forces, enabling both flexion and ab/adduction motions while enhancing fingertip force. Furthermore, to maximize fingertip force, the Force-Enhanced Pleated (FEP) mechanism was applied to the chambers, increasing force by 32.41% compared to conventional chamber designs. The proposed SOFRo Gripper achieves a high fingertip force of 68.76 N and dexterous motion capabilities, enabling a maximum lifting force of 400.0 N and in-hand manipulation. To validate its versatility, extensive experiments were conducted, demonstrating the hand's capability to perform a wide range of tasks. As a result, the SOFRo Gripper successfully performed grasping tasks involving various objects, as well as high-force tasks (e.g., lifting heavy objects, closing a valve), delicate tasks (e.g., grasping tofu, inserting a light bulb), and high-speed tasks (e.g., spinning a top, catching a ball). The system demonstrates high force capability and performs a wide range of tasks.**

***Index Terms*—Soft pneumatic actuator, Soft robotic Gripper, Multi-degree-of-freedom manipulation, Adaptive manipulation**

I. INTRODUCTION

ACHIEVING human-like versatility in robotic hands remains a significant challenge in the field of robotics research [1]. The rich sensory capabilities, high degree of freedom (DoF), significant fingertip force, and fast response serve as important factors that contribute to the versatility of human hands [2]. Many studies have aimed to replicate these features, particularly focusing on achieving multi-DoF, and have developed robotic hands that mimic the structure and versatility of human hands [3], [4]. However, using an excessive number of actuators and sensors introduces several challenges, including increased system and control complexity, high costs, transmission losses, and reduced force density [5].

To address these challenges, researchers have focused on developing soft robotic hands that leverage soft actuators with compliant characteristics [6]. Among these approaches, soft grippers actuated by pneumatic actuators have simplified systems while enabling versatile grasping based on compliance [7], [8]. As a result, researchers have developed a soft gripper capable of reliably grasping various objects without significant effort in control. However, these soft grippers often follow predefined trajectories set during the design process, limiting their functionality to only grasping tasks [9], [10].

One approach to addressing these functional limitations is to expand the DoF of soft robotic hands. Increasing the DoF offers numerous advantages, including improved grasping stability and added ability to perform in-hand manipulation [11]. To achieve this, researchers have increased the DoF by integrating multiple chambers in an antagonistic configuration [12]. As a result, they have developed soft robotic hands composed of finger modules with higher DoF, enabling a wider range of tasks through multi-DoF motions. Other studies have increased DoF by employing additional actuators, such as motors, alongside soft pneumatic actuators [13]. While these approaches have effectively improved the dexterity and range of motions of soft robotic hands, other important factors, such as generating sufficient fingertip force, are often overlooked. To design a versatile robotic hand, researchers must simultaneously consider fingertip force and multi-DoF motion [14]. However, despite these efforts, most robotic hands still lack sufficient force to perform a wide range of tasks comparable to those of the human hand.

We developed the Soft Omni-Functional Robotic Gripper (SOFRo Gripper) to enhance versatility by integrating high grasping force and multi-DoF motion. The SOFRo Gripper is composed of the Synergistic Chamber Finger Module (SCFM), which enhances force, speed, and DoF in the flexion direction by coordinating three chambers arranged synergistically in Fig. 1. Additionally, the SCFM provides ab/adduction motions and employs a multi-node tendon routing strategy, further improving the dexterity and force

Singyoung Lee, Genesung Kang, Hongmin Kim and Dongjun Shin are associated with the Yonsei University, Seoul, 03722, South Korea (e-mail: tlsdud1324@gmail.com gsk808@yonsei.ac.kr; hm@yonsei.ac.kr; dj.shin@yonsei.ac.kr). (Corresponding author: Dongjun Shin.)

This work was supported by the Industrial Strategic Technology Development Program funded by the Ministry of Trade, Industry & Energy (MOTIE, Korea) and the Korea Evaluation Institute of Industrial Technology (KEIT) under Grant No. 20007058 (Development of safe and comfortable human augmentation hybrid robot suit) and Grant No. RS-2024-00444294 (Development of Core Technologies for a Multi-Drive Robot Platform Capable of Performing Tasks in Military Areas with Uneven Terrains). (Sinyoung Lee and Genesung Kang contributed equally to this work.)

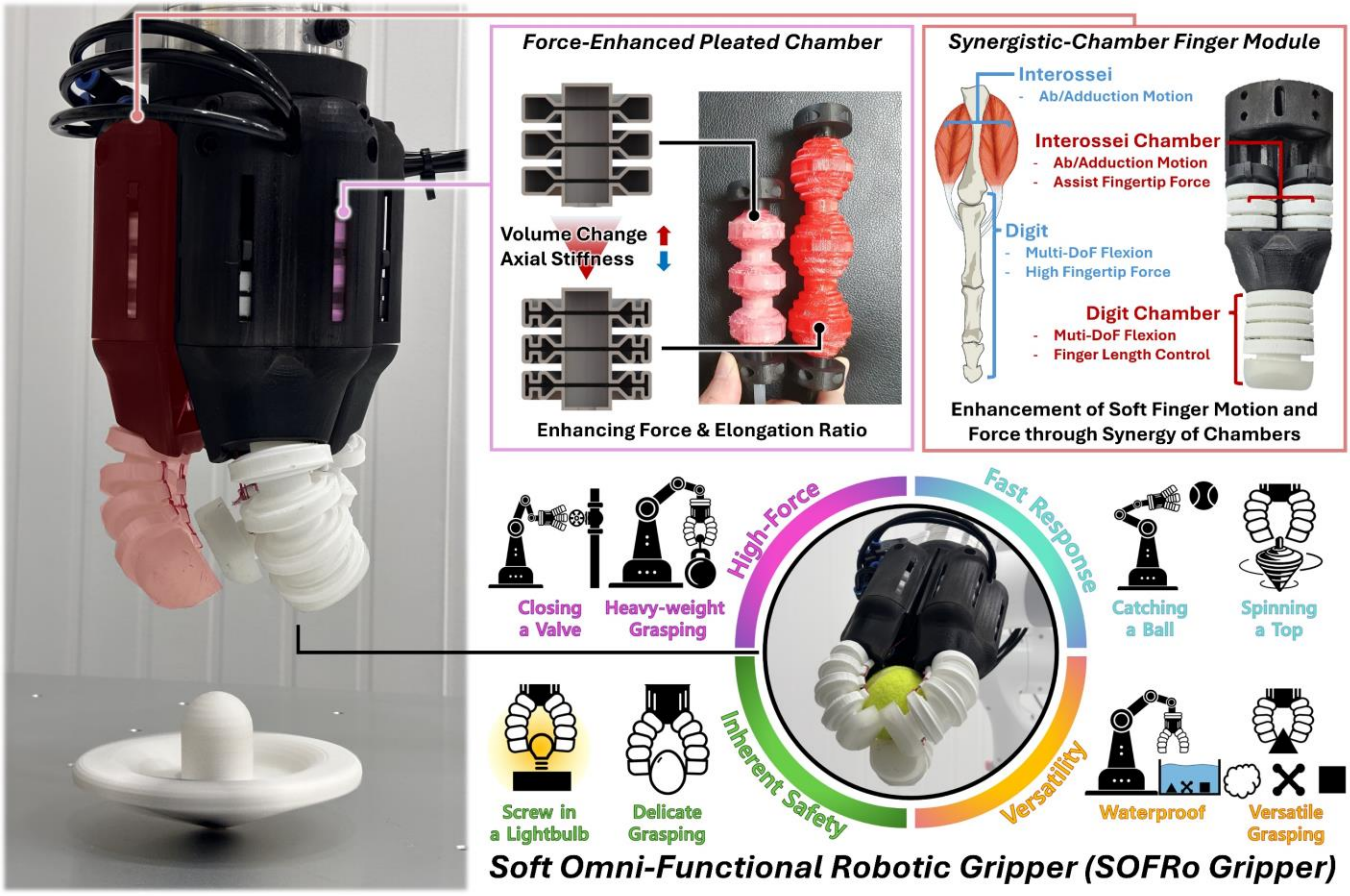

Fig. 1. Overview of the Soft Omni-Functional Robotic Gripper (SOFRo Gripper) and its applicable tasks. The SOFRo Gripper consists of nine chambers integrated with the Force-Enhanced Pleated (FEP) mechanism, which are strategically arranged to provide multi-DoF motion for each finger. Additionally, the chamber configuration is designed to generate high fingertip force in the flexion direction, enabling enhanced performance in various manipulation tasks

transmission of the pneumatic finger. The SCFM incorporates a Force-Enhancing Pleated (FEP) mechanism into its chambers to increase both the expansion force and expansion ratio, thereby generating greater fingertip force. As a result, the SOFRo Gripper, which consists of SCFMs capable of multi-DoF motion with high force, performs various tasks—from those requiring high force output to those demanding rapid actuation and delicate handling of fragile materials.

II. Design of Soft Omni-Functional Robotic Gripper

The human finger evolved to enhance its flexion capability for tool use. It enables dexterous movement through its DoF in abduction and adduction, as well as multi-DoF motion in the flexion direction [15]. Additionally, a typical adult human hand exhibits a high grip force of approximately 30–50 kgf [16] and a rapid flexion response time of about 140–160 ms [17]. These characteristics provide significant advantages in tool manipulation and the execution of various tasks.

Inspired by these characteristics, we designed the SOFRo Gripper to improve flexion functionality by enhancing DoF, fingertip force, and actuation speed. The SOFRo Gripper comprises three SCFMs, each consisting of three pneumatic chambers.

A. Synergistic-Chamber Finger Module (SCFM) Design

As shown in Fig. 2(A), the SCFM includes two components—the Digit Chamber and the Interossei Chamber, and the overall size and geometric layout of the fabricated module can be identified from the schematic shown at the top of Fig. 2(A). The Digit Chamber allows finger length modulation and multi-DoF flexion, thereby improving grasping effectiveness. In parallel, the Interossei Chamber enhances fingertip force during flexion while enabling abduction and adduction, improving overall finger dexterity. To further enhance fingertip force, a Force-Enhanced Pleated (FEP) mechanism was applied to the cross-sectional design of the Interossei Chambers. Further details on the structure and function of the FEP mechanism are provided in the next subsection.

As shown in Fig. 2(B), the SCFM exhibits different motions depending on the pressure combinations applied to the chambers. When pressure is applied to the right Interossei Chamber together with the Digit Chamber, flexion and abduction occur. Conversely, when pressure is applied to the left Interossei Chamber and the Digit Chamber, flexion and adduction are generated. When only the Interossei Chambers are pressurized, the module maintains its shape without noticeable bending. Subsequently applying pressure to the Digit Chamber produces a high-curvature bending motion. In contrast, when the Digit

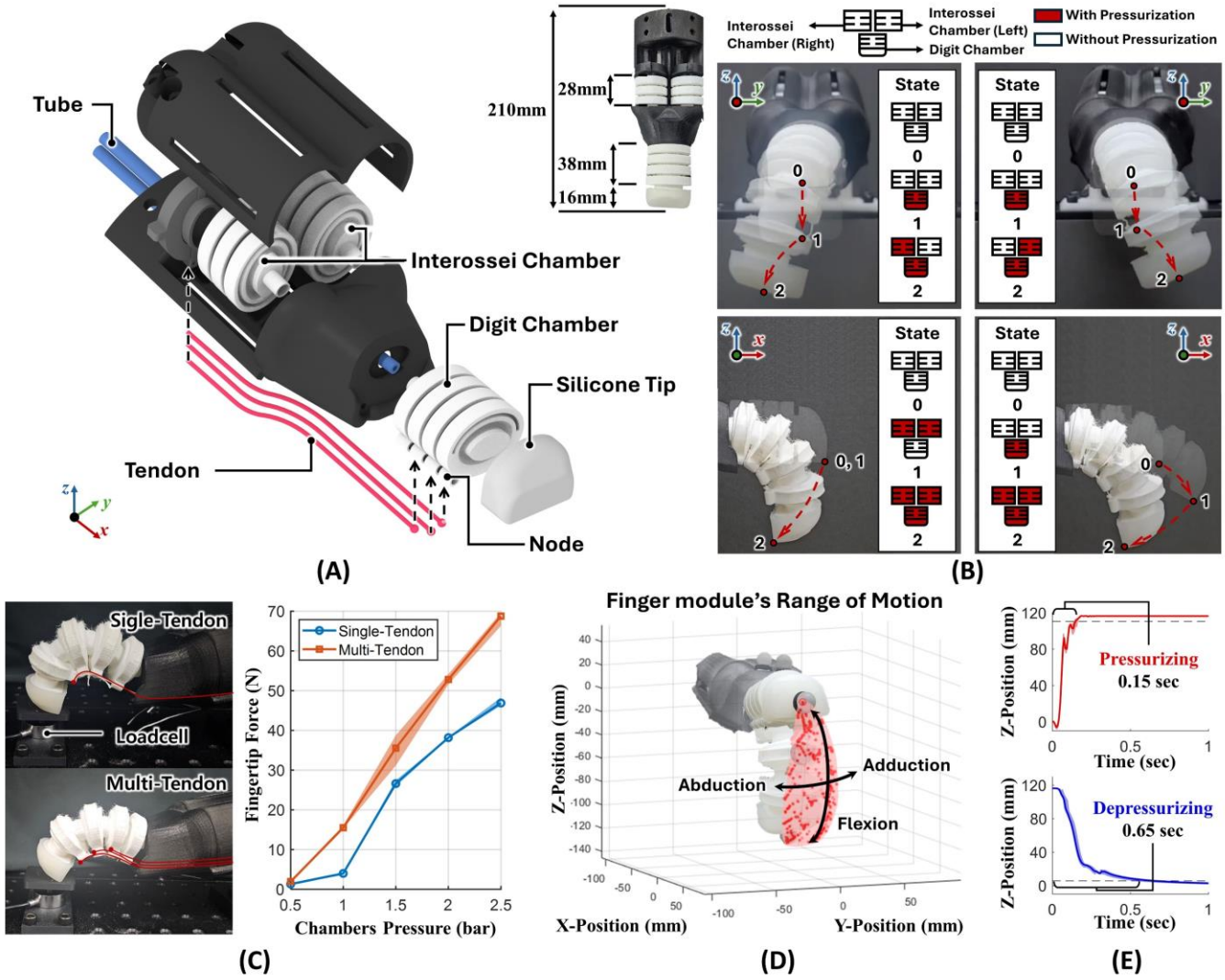

Fig. 2. Overview of the Synergistic-Chamber Finger Module (SCFM) and its characteristics. (A) Structural composition of the SCFM. (B) Motion of the SCFM in response to chamber pressures. (C) Experimental setup and results of fingertip force measurement under different Tendon routing conditions. (D) Range of Motion (RoM) of the SCFM. (E) Graph showing the actuation time required for maximum flexion and release.

Chamber is pressurized first, a low-curvature bending motion initially occurs due to expansion, and additional pressurization of the Interossei Chambers increases the bending curvature.

During deformation of the Digit Chamber, buckling can reduce bending force. To mitigate this, tendons were connected to all nodes except for the first node, where deformation was minimal, resulting in six tendons per Digit Chamber. This configuration distributes the force from the Interossei Chamber evenly across the nodes, reducing buckling and increasing bending force compared to the conventional design with a single tendon fixed only at the fingertip, as shown in Fig. 2(A). For experimental validation, the finger module was fixed as shown in Fig. 2(C). No external constraints were applied to the Digit Chamber, and all chambers were pressurized uniformly using a pneumatic regulator. The pressure was increased from 0.5 to 2.5 bar in 0.5 bar increments, and the fingertip force was measured five times at each state. As shown in Fig. 2(C), the proposed tendon configuration achieved a maximum fingertip force of 68.76 N at 2.5 bar, while the single-tendon configuration produced 48.88 N under the same conditions.

To specifically evaluate the performance of the SCFM, we conducted experiments to measure its range of motion (RoM), actuation speed, and fingertip force. The experiment utilized an optical marker-based motion capture system (V120 Trio; OptiTrack, NaturalPoint Inc.) to measure the range of motion and actuation speed. The experimental results are presented as graphs in Figs. 2(D) and (E), where Fig. 2(D) illustrates the SCFM's RoM, and Fig. 2(E) shows the measured actuation speed. For the RoM measurement, the position data of a marker attached to the fingertip were recorded under different combinations of chamber pressures. The pressure combinations were varied from 0.1 to 2.5 bar in increments of 0.2 bar. The actuation speed assessment measured the time required for the SCFM to achieve maximum flexion when pressurized from 0 bar to 2.5 bar under a step input. The chamber pressures were controlled using a pneumatic regulator. Additionally, the test measured the time required for the module to return to its initial position after completing full flexion. The results represent the mean values from seven trials. Specifically, the experiment measured the time required to reach 95% of the final

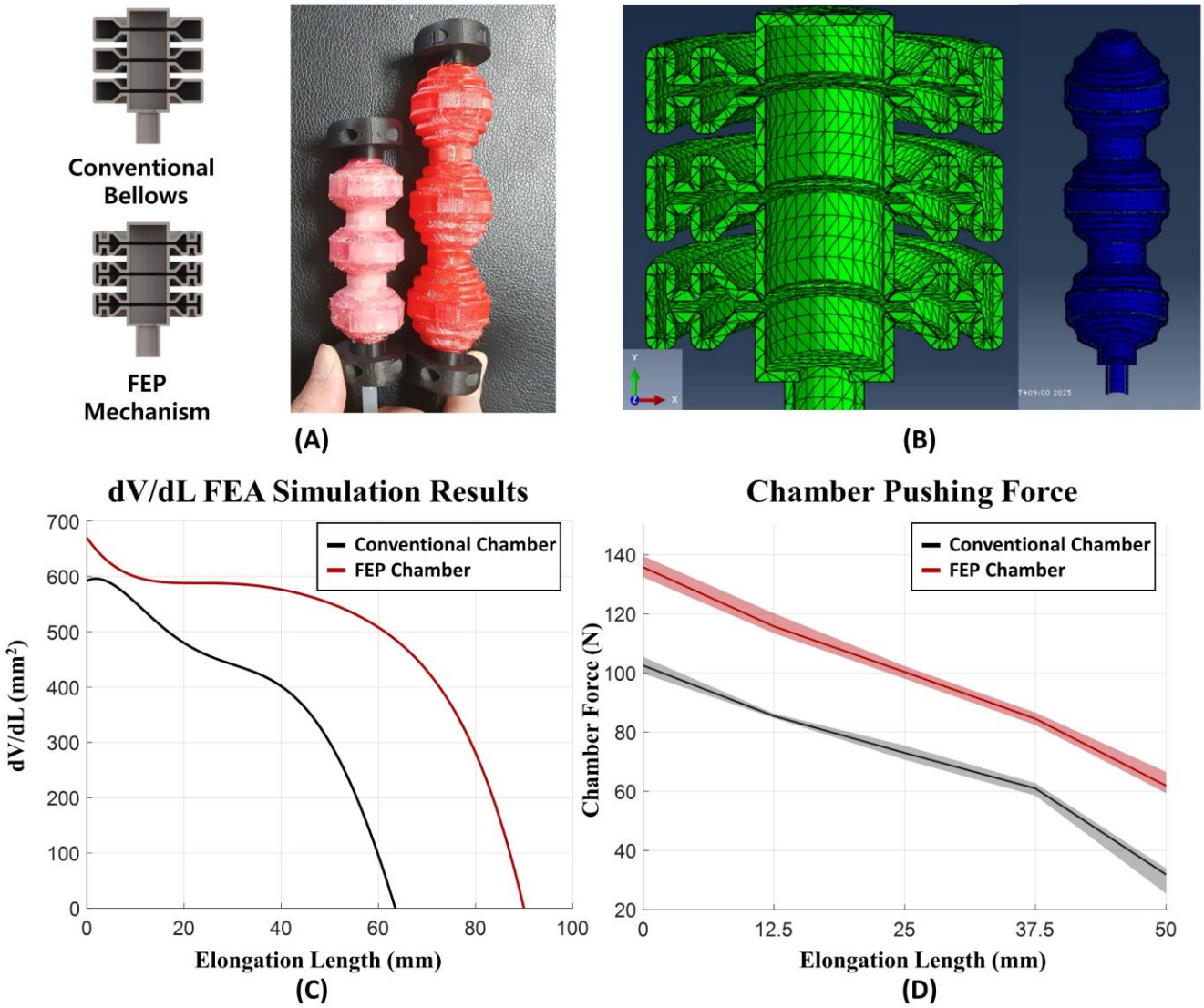

Fig. 3. Comparison of the structural characteristics. (A) Actuating picture of Conventional Chamber and the Force-Enhanced Pleated (FEP) Chamber. (B) is picture of the FEA Simulation. (C) Graph comparing the volume-to-length derivative of the Conventional Chamber and the FEP Chamber. (D) Chamber force comparison graph at 2 bar.

displacement. The results indicate that the SCFM achieved maximum flexion in approximately 0.15 seconds and returned to its original position within 0.65 seconds, demonstrating rapid responsiveness suitable for dynamic tasks.

B. Force-Enhanced Pleated Chamber Design

The expansion force of chambers, such as the one shown in Fig. 3 (A), that actuate through volumetric expansion is calculated based on the principle of virtual work.

$$\delta W_{out} = \delta W_{in} \tag{1}$$

$$(F_{chamber} + F_{restoring})dL = (P_{chamber} - P_{atm})dV \tag{2}$$

$$F_{chamber} = (P_{chamber} - P_{atm})\frac{dV}{dL} - F_{restoring} \tag{3}$$

Here, W_{out} represents the work by the chamber, W_{in} denotes the work by the air pressure, $F_{chamber}$ is the force exerted by the chamber, and $F_{restoring}$ refers to the restoring force of the chamber. $P_{chamber}$ and P_{atm} represent the internal pressure of the chamber and atmospheric pressure, respectively. V denotes the volume of the chamber, while L represents the expansion length of the chamber.

According to Eq (3), a higher $P_{chamber}$ and a larger dV/dL result in an increased expansion force. To increase the pressure limit of the chamber, the Interossei Chamber was designed to operate through structural deformation rather than material deformation. Actuators utilizing this approach can withstand higher pressures, achieve faster actuation speeds, and generate greater force compared to those using hyper-elastic materials [18], [19]. Therefore, instead of hyper-elastic materials, high-hardness thermoplastic polyurethane (95A TPU) with lower strain was selected to increase the maximum pressure limit of the chamber.

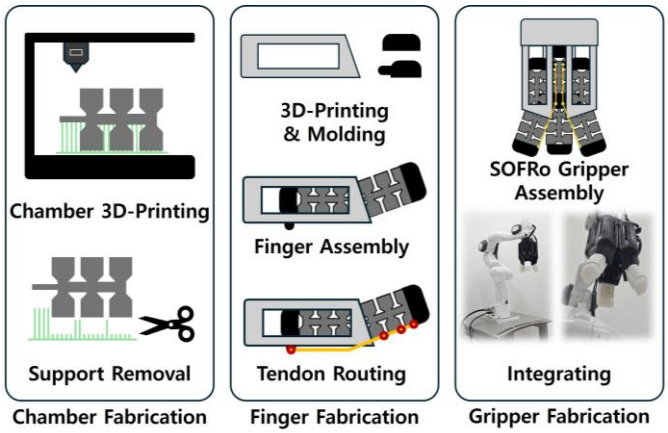

Fig. 4. Fabrication process of the Soft Omni-Functional Robotic (SOFRo) Gripper

Additionally, to increase dV/dL and reduce $F_{restoring}$, pleats were added to the bellows-based cross-section, enabling greater volume change per length change. As shown in Fig. 3, finite element analysis (FEA) was conducted to analyze volume and length variations depending on cross-sectional patterns, leading to the fabrication of an actuator with improved expansion force and expansion ratio. As shown in Fig. 3 (D), the chamber with the FEP mechanism exhibited a 32.41% increase in maximum force compared to the conventional chamber under a pressure of 2.0 bar. However, it remained susceptible to buckling. To mitigate the effects of buckling, the chamber was enclosed within a case when applied to the actual SCFM, providing guidance in the expansion direction. Detailed information on the chamber modeling is provided in Supplementary S3–S8.

Adjusting finger length provides advantages in grasping performance by allowing for more adaptable interactions with objects. To achieve this, the Digit Chamber was designed to expand while maintaining its own curvature, enabling dynamic length adjustment. A method for inducing chamber curvature is to create asymmetric length variations at the same pressure level, which can be achieved through asymmetric thickness, eccentricity, or differences in cross-sectional patterns. Among these approaches, asymmetric thickness provides better control over curvature but results in a reduced expansion ratio. Eccentricity, on the other hand, offers both higher curvature and expansion ratio but increases susceptibility to buckling, limiting its practical application. Considering these trade-offs, the Digit Chamber was designed by incorporating differences in cross-sectional patterns, allowing for effective curvature generation while maintaining structural stability and expansion efficiency.

III. Fabrication

The fabrication process involves manufacturing and assembling the components of the finger module, which is then integrated into a robot arm (FR3; Franka Robotics GmbH), as shown in Fig. 4. We fabricated the chambers using Skin 30 (Smooth-On Inc.), and the black enclosure housing a 3D printer, and the chamber material was 95A TPU. Fabrication of the fingertip involved molding with Dragon the chambers was fabricated using a selective laser sintering (SLS) 3D printer (Fuse 1+; Formlabs). After fabricating the individual components, they were assembled to construct the SCFM. For force transmission, high-performance wires (452Xtra Bowstring; BCY Inc.) containing Dyneema SK75 fibers were used, providing excellent thermal stability, chemical resistance, fatigue resistance, and high mechanical strength. The tendons were connected to all nodes of the Digit Chamber except for the first node, where deformation was minimal, resulting in a total of six tendons per finger. The tendon lengths were individually adjusted considering the maximum deformation of the Interossei Chamber. Finally, three identical SCFM units were mounted onto a fixture to complete the SOFRo Gripper, which was subsequently integrated into the robot arm.

IV. Experiments

A. Stiffness and Durability Tests

The stiffness and durability of the finger module were experimentally evaluated, as shown in Fig. 5. For the stiffness measurement, as shown in Fig. 5(A), a handle was attached to a force gauge (DGT-100; DigiTech Co., LTD). While pressure was applied to the actuator, the fingertip pressed the handle, and the force gauge was gradually moved upward to measure the reaction force. The stiffness was calculated from the measured force–displacement relationship, and the corresponding results are presented in Fig. 5(B). Each test was repeated five times under the same conditions, and the results in the graph represent the mean values.

In addition, for the durability test, as shown in Fig. 5(A), the finger module was fixed, and the actuator was repeatedly pressurized and exhausted at 2-second intervals while measuring the contact force using a load cell. The durability test results indicate the relationship between pressure and the number of operation cycles (Supplementary Fig. S9). At 1.0 bar, a slight air leakage was first observed after approximately 7,410 cycles, but no significant degradation in performance was detected. At 1.5 bar, minor leakage began around 4,220 cycles; however, performance remained stable up to 10,000 cycles. At 2.0 bar, air leakage started at around 935 cycles, and a noticeable decline in performance occurred after approximately 1,400 cycles. The leakage primarily occurred in the Digit Chamber, where large deformation was concentrated, whereas no damage was observed in the tendons or other components throughout 10,000 cycles of operation.

B. Force and Torque Evaluation

This subsection evaluates the performance of the SOFRo Gripper, which incorporates three SCFMs, by measuring its lifting force and torque. Experiment determines the maximum force using a force gauge, as shown in Fig. 5 (C) and (D). The lifting force experiment involves gripping a cylindrical handle attached to the force gauge via a steel wire to measure the maximum force exerted by the SOFRo Gripper to lift the handle.

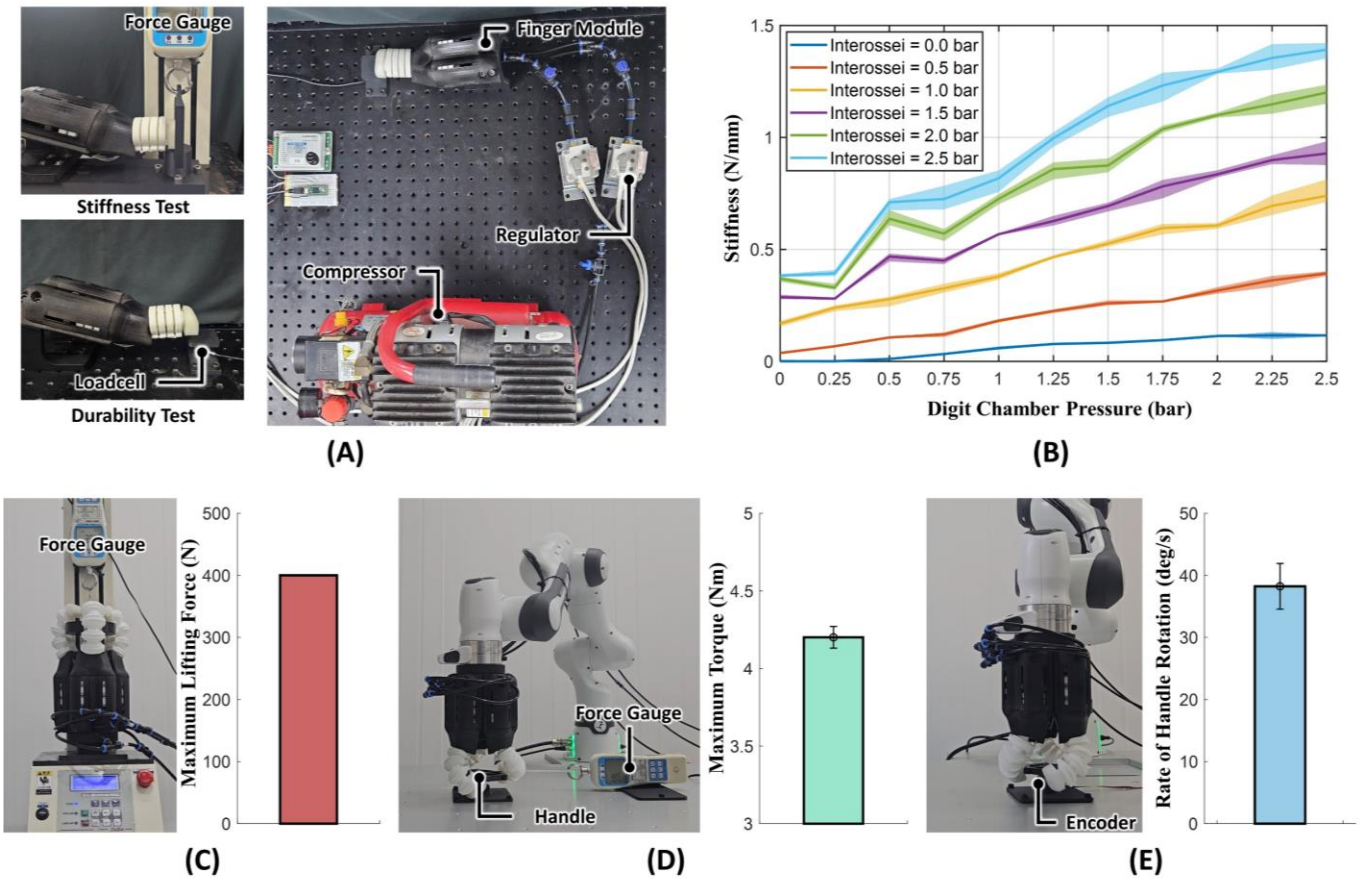

Fig. 5. Force and Torque evaluation of the Finger module and SOFRo gripper. (A) Experimental setup of the finger module. (B) Results of the bending-direction stiffness test. (C) Experimental result of maximum lifting force measurement. (D) Experimental result of maximum torque measurement while gripping a valve wheel. (E) Experimental result of rotation speed measurement for turning a valve wheel.

The experiment uses a cylindrical handle with a radius of 50 mm and a height of 30 mm. When each chamber is pressurized to 2.5 bar pressure while maintaining its grasp, the lifting force reaches a maximum of 400 N, which may vary depending on the interaction scenario. The maximum force was measured until the SOFRo Gripper experienced structural failure and could no longer retain its grasp on the handle. Due to the destructive nature of the experiment, it was conducted only once.

The torque measurement experiment uses a valve wheel with a radius of 50 mm. A steel wire connects the valve wheel to the force gauge, and the maximum force exerted by the SOFRo Gripper while attempting to rotate the valve wheel is measured to calculate the torque. Among the seven repeated trials, the maximum force recorded by the force gauge is 89.5 N, corresponding to a torque of approximately 4.475 Nm. The result, calculated as the average of the five remaining values after excluding the maximum and minimum, is approximately 4.20 Nm. This result is presented in Fig. 5 (D).

The valve wheel rotation speed experiment evaluates the SOFRo Gripper's ability to rotate the valve wheel based on the actuation speed measured in Fig. 5 (E). This experiment uses the same valve wheel as in the torque measurement test. The rotation angle of the valve wheel is measured using an absolute encoder (SME360AP-05DP, SERA Co., Ltd.). The average angular velocity is calculated based on the total rotation angle and the time taken over ten actuation commands. The results indicate that the SOFRo Gripper rotates the valve wheel at an angular velocity of approximately 38.24 deg/sec. This value is the average obtained from seven repeated measurements. Reducing the pressurizing and exhaust times compared to the above experiment frequently disrupts the rotational motion, either preventing the valve wheel from rotating or causing it to reverse after rotation. Consequently, the angular velocity decreases. Conversely, increasing the pressurizing and exhaust times prolongs the overall actuation time, leading to a reduction in the valve wheel's angular velocity.

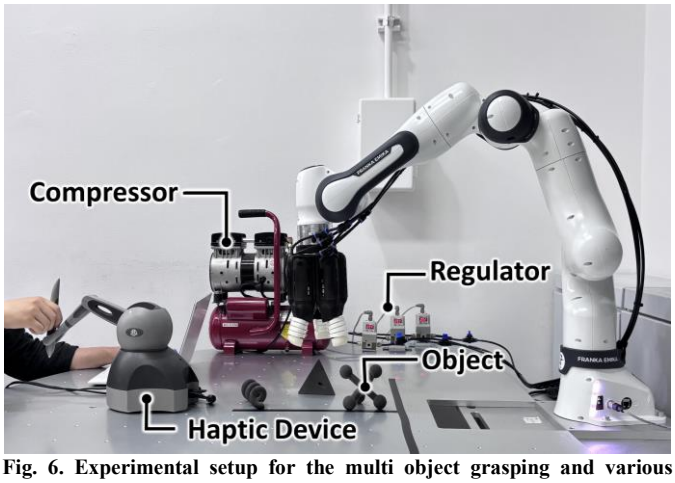

Fig. 6. Experimental setup for the multi object grasping and various manipulation task.

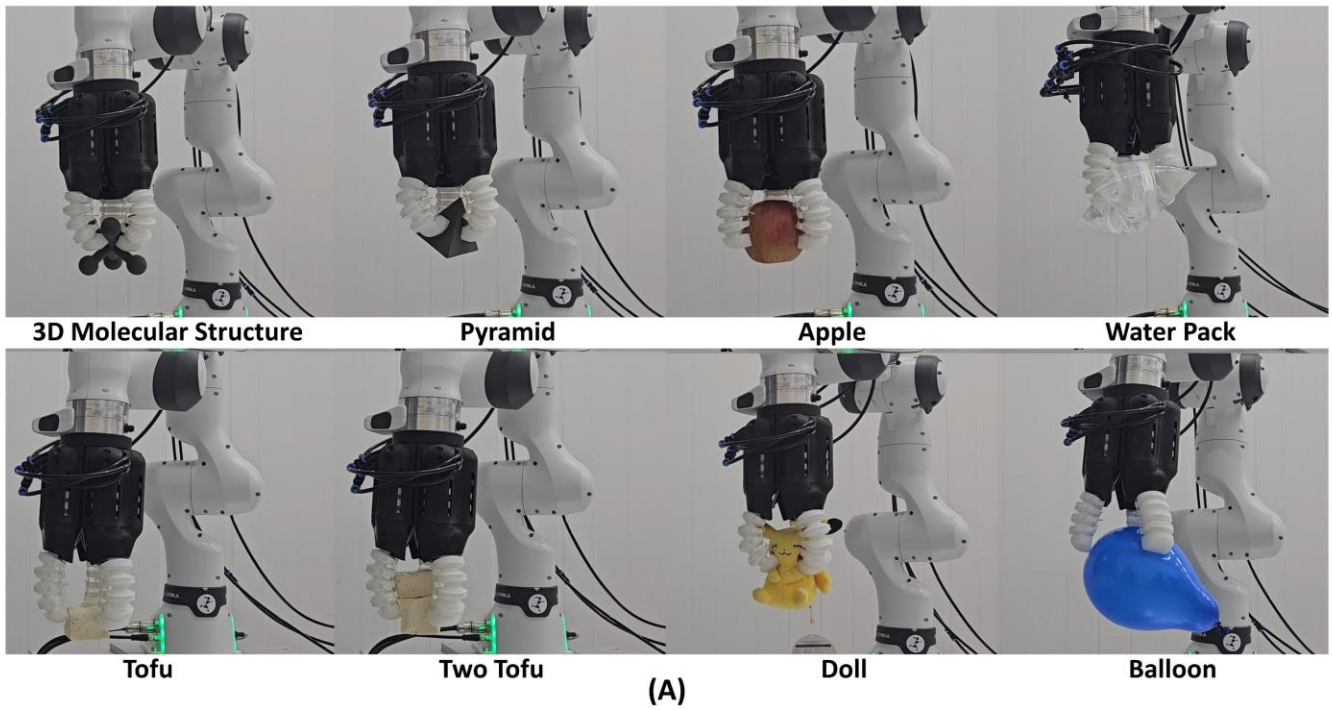

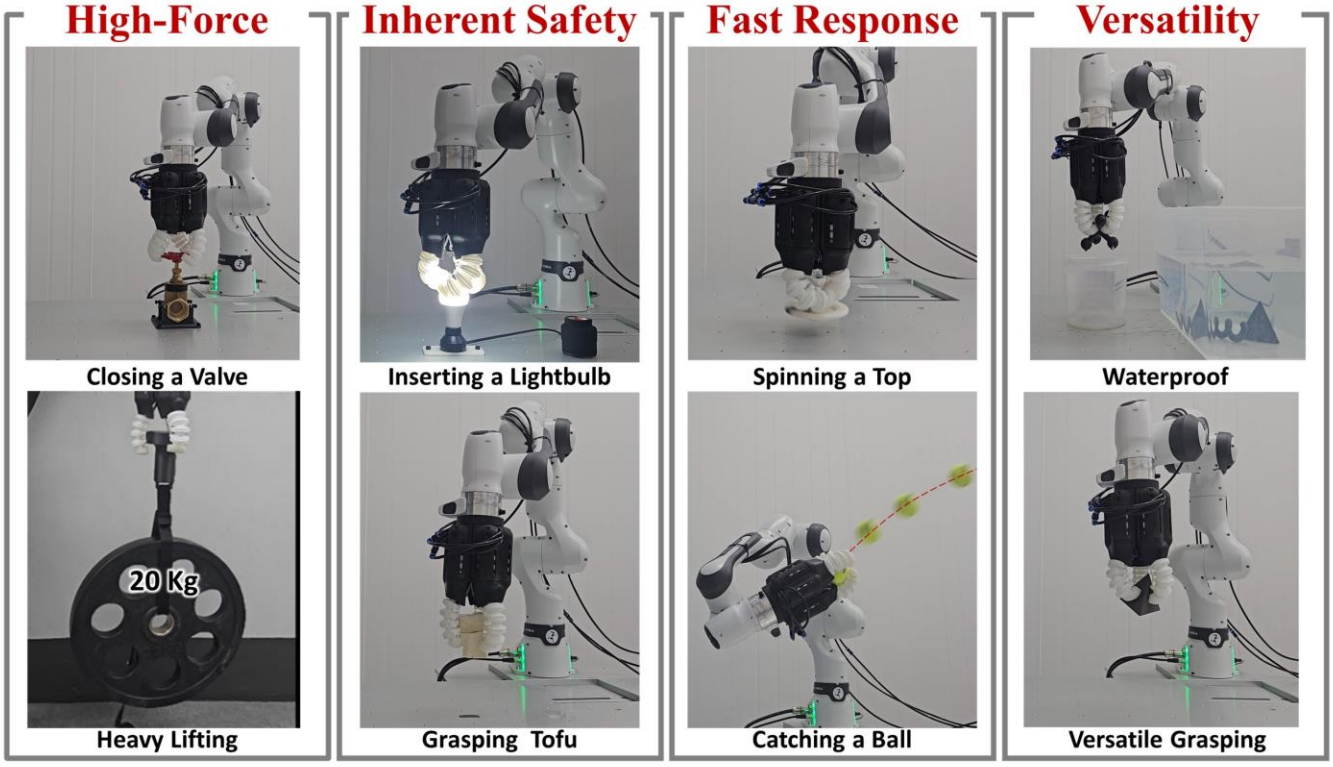

Fig. 7. Demonstration of the SOFRo Gripper's versatility in performing various tasks. (A) Grasping performance demonstrated by lifting various objects. (B) Shows the SOFRo Gripper executing a wide range of tasks, from high-force tasks to delicate and rapid-response tasks.

C. Grasping and Manipulation

To enable the execution of various grasping and manipulation tasks, the experimental setup was configured as shown in Fig. 6. The pressures of the nine chambers integrated into the SOFRo Gripper were controlled using pneumatic regulators (ITV2050; SMC Corp.), which supplied and maintained the desired pressure levels. A microcontroller unit (Teensy 4.1; PJRC) was used to process real-time sensor data collected during the experiments and to generate appropriate control signals for the pneumatic regulators, ensuring stable and responsive actuation. The robot arm was connected to a haptic device (Touch X; 3D Systems Inc.), allowing an operator to intuitively control the Gripper's movements while receiving visual feedback from the experimental environment.

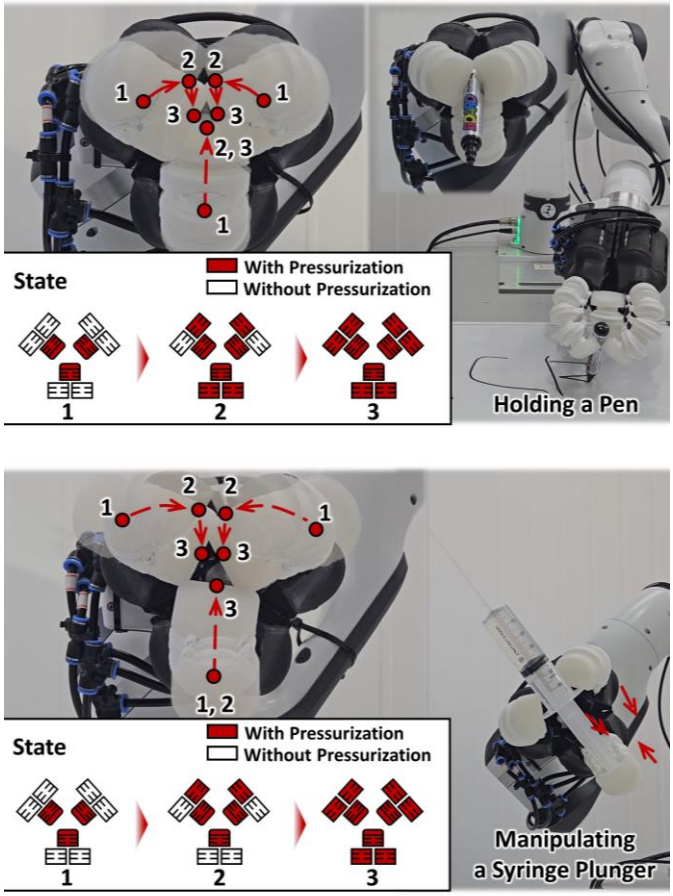

Fig. 8. Demonstration of the SOFRo Gripper's versatility in performing various tasks. (A) and (B) show the use of different tools, such as a pen and a syringe, enabled by modifying the chamber connections.

As shown in Fig. 7, the SOFRo Gripper can grasp various objects and perform tasks, including those requiring high force (e.g., closing a valve, lifting a heavy object), delicate handling (e.g., inserting a light bulb, grasping tofu), fast actuation speed (e.g., spinning a top, catching a ball), and versatility (e.g., waterproof, versatile grasping). Notably, even delicate items like tofu, which typically deform under external forces, were grasped without noticeable deformation. The tofu-grasping experiment was conducted based on the force values reported in [20], which defined the required grasping force for stable tofu handling. These diverse grasping and manipulation tasks are enabled through appropriate combinations of pressures across the Digit and Interossei Chambers, allowing the gripper to transition between high-force and highly compliant grasp configurations depending on task requirements, rather than relying on precise regulation of a single contact force.

The SOFRo Gripper can also perform various dexterous tasks. As shown in Fig. 8(A), one finger can act as a support while the others securely pinch objects such as a pen, resembling how humans hold a pen. Similarly, as illustrated in Fig. 8(B), the gripper can modulate force after grasping, such as controlling the applied force when pressing a syringe. These examples demonstrate the gripper's ability to perform diverse and adaptive manipulation tasks, as shown in Videos S1–S6.

Conventional soft grippers lack sufficient degrees of freedom to perform various in-hand manipulation tasks. Existing soft robotic hands also have difficulty performing high-force tasks due to limited grasping force. The SOFRo Gripper performs all these tasks based on its high fingertip force and multi-DoF motion. A comparison with existing soft grippers and robotic hands is provided in the Supplementary Material (Table S1-S2).

V. Conclusion

This study proposes the SOFRo Gripper, which achieves high force capacity and multi-DoF motion through the application of a FEP mechanism in the chambers and the synergistic arrangement of multiple chambers. The FEP mechanism is applied in chamber design to increase volume change while reducing axial stiffness. As a result, the chamber exhibits a high expansion ratio while increasing expansion force. In the SCFM, the Interossei Chambers and Digit Chamber are strategically integrated. The Interossei Chambers not only provide additional DoF in the abduction/adduction direction but also assist in generating fingertip force in the flexion direction. Additionally, the Digit Chamber enables finger length variation and multi-DoF flexion, enhancing grip stability when grasping objects. The SOFRo Gripper, integrating these mechanisms, not only generates a maximum lifting force of 400 N but also performs a variety of tasks based on its multi-DoF capabilities, as demonstrated through experiments. To the best of our knowledge, no previous gripper has achieved high output force and multi-DoF manipulation simultaneously without using a braking mechanism. The proposed SOFRo Gripper demonstrates the potential of combining high force capacity and dexterous motion within a single soft robotic system. Building on these results, future work will further explore this direction, emphasizing that achieving human-like manipulation requires both strength and dexterity.

In parallel, the SOFRo Gripper currently weighs 1.02 kg, including 108.4 g from the nine chambers. Future development will focus on refining the finger dimensions and overall configuration to achieve a more compact and human-like robotic hand while maintaining high force capability and multi-DoF performance. These advancements are expected to further enhance the practicality and applicability of the SOFRo Gripper.

References

[1] C. Piazza, G. Grioli, M. G. Catalano, and A. Bicchi, "A century of robotic hands," *Annu. Rev. Control Robot. Auton. Syst.*, vol. 2, no. 1, pp. 1–32, May. 2019, doi: 10.1146/annurev-control-060117-105003.

[2] T. Ren et al., "Novel bionic soft robotic hand with dexterous deformation and reliable grasping," *IEEE Trans. Instrum. Meas.*, vol. 72, pp. 1–10, Feb. 2023, doi: 10.1109/TIM.2023.3248098.

[3] P. Tuffield and H. Elias, "The shadow robot mimics human actions," *Ind. Robot*, vol. 30, no. 1, pp. 56–60, Feb. 2003, doi: 10.1108/01439910310 457715.

[4] J.-H. Bae, S.-W. Park, J.-H. Park, M.-H. Baeg, D. Kim, and S.-R. Oh, "Development of a low cost anthropomorphic robot hand with high capability," *In 2012 IEEE/RSJ International Conference on Intelligent Robots and System*, Vilamoura-Algarve, Portugal, Oct. 2012, pp. 4776–4782.

[5] J. Shintake, V. Cacucciolo, D. Floreano, and H. Shea, "Soft robotic grippers," *Adv. Mater.*, vol. 30, no. 29 1707035, May. 2018, doi: 10.1002/adma.201707035.

[6] L. Liu, J. Zhang, G. Liu, Z. Zhu, Q. Hu and P. Li, "Three-fingered soft pneumatic gripper integrating joint-tuning capability," *Soft Robot.*, vol. 9, no. 5, pp. 948–959, Oct. 2022, doi: 10.1089/soro.2021.0082.

[7] D. Mei et al., "Blue hand: A novel type of soft anthropomorphic hand based on pneumatic series-parallel mechanism," *IEEE Robot. Autom.*

Lett., vol. 8, no. 11, pp. 7615–7622, Nov. 2023, doi: 10.1109/LRA.2023.3 320906.

[8] K. R. Kim, S. H. Jeong, P. Kim, and K. S. Kim, "Design of robot hand with pneumatic dual-mode actuation mechanism powered by chemical gas generation method," *IEEE Robot. Autom. Lett.*, vol. 3, no. 4, pp. 4193–4200, Oct. 2018, doi: 10.1109/LRA.2018.2853763.

[9] T. Hao, H. Xiao, S. Liu, C. Zhang and H. Ma, "Multijointed pneumatic soft hand with flexible thenar," *Soft Robot.*, vol. 9, no.4, pp. 745–753, Aug. 2022, doi: 10.1089/soro.2021.0017.

[10] W. Zhu et al., "A soft-rigid hybrid gripper with lateral compliance and dexterous in-hand manipulation," *IEEE/ASME Trans. Mechatron.*, vol. 28, no. 1, pp. 104–115, Feb. 2023, doi: 10.1109/TMECH.2022.3195985.

[11] S. Abondance, C. B. Teeple, and R. J. Wood, "A dexterous soft robotic hand for delicate in-hand manipulation," *IEEE Robot. Autom. Lett.*, vol. 5, no. 4, pp. 5502–5509, Oct. 2020, doi: 10.1109/LRA.2020.3007411.

[12] D. Drotman, M. Ishida, S. Jadhav, and M. T. Tolley, "Application-driven design of soft, 3-D printed, pneumatic actuators with bellows," *IEEE/ASME Trans. Mechatron.*, vol. 24, no. 1, pp. 78–87, Feb. 2019, doi: 10.1109/TMECH.2018.2879299.

[13] D. C. Y. Wong, M. Li, S. Kang, L. Luo and H. Yu, "Reconfigurable, transformable soft pneumatic actuator with tunable three-dimensional deformations for dexterous soft robotics applications," *Soft Robot.*, vol. 12, no. 2, pp. 228-241, Apr. 2025, doi: 10.1089/soro.2023.0072.

[14] M. S. Xavier et al., "Soft pneumatic actuators: A review of design, fabrication, modeling, sensing, control and applications," *IEEE Access*, vol. 10, pp. 59442–59485, Jun. 2022, doi: 10.1109/ACCESS.2022. 3179589.

[15] T. L. Kivell et al., "Form, function and evolution of the human hand," *Am. J. Biol. Anthropol.*, vol. 181, pp. 6–57, Dec. 2022, doi: 10.1002/ajpa. 24667.

[16] G. R. Tomkinson et al., "International norms for adult handgrip strength: A systematic review of data on 2.4 million adults aged 20 to 100+ years from 69 countries and regions," *J. Sport Health Sci.*, vol. 14, 101014, 2024, doi: 10.1016/j.jshs.2024.101014.

[17] X. Li, R. Wen, D. Duanmu, W. Huang, K. Wan and Y. Hu "Finger kinematics during human hand grip and release," *Biomimetics*, vol. 8, no. 2, pp. 244, Jun. 2023, doi: 10.3390/biomimetics8020244.

[18] K. Han, N. Kim, and D. Shin, "A novel soft pneumatic artificial muscle with high-contraction ratio," *Soft Robot.*, vol. 5, no. 5, pp. 554–566, Oct. 2018, doi: 10.1089/soro.2017.0114.

[19] Z. Zhang et al., "Soft and lightweight fabric enables powerful and high-range pneumatic actuation," *Sci. Adv.*, vol. 9, no. 15, eadg1203, Apr. 2023, doi: 10.1126/sciadv.adg1203.

[20] T. Nishimura, Y. Fujihira, R. Adachi, and T. Watanabe, "New condition for tofu stable grasping with fluid fingertips," *In Proc. IEEE Int. Conf. Autom. Sci. Eng. (CASE)*, Fort Worth, TX, USA, Aug. 2016, pp. 335–341.

Sinyoung Lee received M.S. and Ph.D. degrees in mechanical engineering from Chung-Ang University, Seoul, South Korea, in 2019 and 2025, respectively. He is currently a Postdoctoral Researcher in the Department of Mechanical Engineering at Yonsei University, Seoul, South Korea. His research interests include design and control of novel bio-inspired mechanisms and soft pneumatic actuators.

Genesung Kang is currently pursuing an integrated M.S./Ph.D. degree in mechanical engineering at Yonsei University, Seoul, South Korea. His research focuses on the design and control of soft pneumatic robots and soft wearable robots for safe human–robot interaction.

Hongmin Kim is currently pursuing an integrated M.S./Ph.D. degree in mechanical engineering at Yonsei University, Seoul, South Korea. His research interests include the design and control of soft grippers and robotic arm manipulation.

Dongjun Shin received M.S. and Ph.D. degrees in mechanical engineering from Stanford University, Stanford, CA, USA, in 2005 and 2011, respectively. He is currently an associate professor with the Department of Mechanical Engineering, Yonsei University, Seoul, South Korea. His research interests include soft robotics and human-friendly robots.